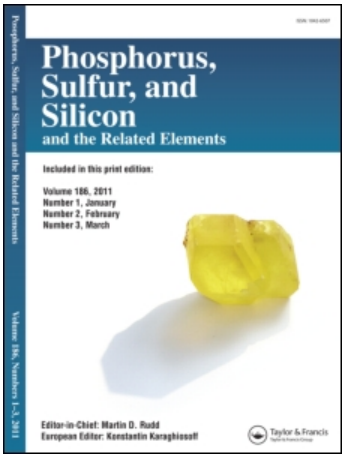

Phosphorus, Sulfur, and Silicon and the Related Elements
Publication details, including instructions for authors and subscription information:
http://www.informaworld.com/smpp/title~content=t713618290

Studies on the Hydrogen Transfer Reaction Mechanism of Singlet Thiol Phosphinidene Complex and the Temperature Effect

Ping Yin[a]; Hou Chen[a]; Chunhua Wang[a]; Qiang Xu[a]; Lei Chen[a]; Chongrong Bao[a]
[a] School of Chemistry and Materials Science, Ludong University, Yantai, P. R. China

Online publication date: 28 December 2009

To cite this Article Yin, Ping , Chen, Hou , Wang, Chunhua , Xu, Qiang , Chen, Lei and Bao, Chongrong(2010) 'Studies on the Hydrogen Transfer Reaction Mechanism of Singlet Thiol Phosphinidene Complex and the Temperature Effect', Phosphorus, Sulfur, and Silicon and the Related Elements, 185: 1, 12 — 21
To link to this Article: DOI: 10.1080/10426500802705578
URL: http://dx.doi.org/10.1080/10426500802705578

Phosphorus, Sulfur, and Silicon, 185:12–21, 2010

ISSN: 1042-6507 print / 1563-5325 online
DOI: 10.1080/10426500802705578

Taylor & Francis
Taylor & Francis Group

STUDIES ON THE HYDROGEN TRANSFER REACTION MECHANISM OF SINGLET THIOL PHOSPHINIDENE COMPLEX AND THE TEMPERATURE EFFECT

Ping Yin, Hou Chen, Chunhua Wang, Qiang Xu, Lei Chen, and Chongrong Bao
School of Chemistry and Materials Science, Ludong University, Yantai, P. R. China

The hydrogen transfer reaction mechanism of the complex of a singlet thiol phosphinidene and a polar molecule hydrogen fluoride (HSP- - - HF) has been investigated at the B3LYP/6-311+G (d,p) level in order to better understand the reactivity of singlet phosphinidene. The results show that the relevant reaction, including step 1 [HSP- - -HF(1) → TS1 (2) → HSPH(F) (3)] and step 2 [HSPH(F) (3) → TS2 (4) → H_2SPF (5)], are very different from the reactions of hydroxyl phosphinidene with hydrogen fluoride. Furthermore, theoretical studies on the thermodynamic and kinetic properties of the reaction have been carried out over the temperature range of 200–1200 K using the DFT/B3LYP method, the general statistical thermodynamics, and Eyring transition state theory with Wigner correction, which is used to examine the temperature effects the reaction channel. It is concluded that step 1 has both thermodynamic and kinetic advantages over step 2, and the high temperature is favorable to step 2. Moreover, the order of lgK and lgk for the steps are consistent with the order of their exoergic energies ΔE and barrier height, but the differences of lg**K** and lg**k** for the steps decrease with the temperature increases.

Keywords DFT; hydrogen transfer reaction mechanism; singlet thiol phosphinidene; temperature effects; thermodynamic and kinetic properties

INTRODUCTION

Recently, increased attention has been focused on the chemistry of phosphinidene, which is the analogue to the better-known carbene, both experimentally and theoretically because it plays an important role in the field of chemical catalysis, elementary chemistry, and organometallic chemistry.[1–4]

Free phosphinidenes are unstable and short-lived, and as such, their experimental information of the thermodynamic and kinetic data is rare due to the difficult preparation.

Received 27 August 2008; accepted 15 December 2008.
We greatly appreciate the support provided by the Promotional Foundation for the Excellent Middle-Aged and Young Scientists of Shandong Province of China (2007BS08027), the Basic Project of Educational Bureau of Shandong Province of China (J07YA16), the Open Experiments Project, and the Foundation of Innovation Team Building of Ludong University (08-CXB001). We also thank Ludong University Dawning HPC Center for some calculations.

Address correspondence to Ping Yin, School of Chemistry and Materials Science, Ludong University, Yantai 264025, P. R. China. E-mail: yinping426@163.com

So far, the relevant research work includes the following: Li et al.[5] reported the detection of the mesitylphosphinidene using ESR spectroscopy, establishing the existence of RP as free transient species. Nguyen et al.[6] found that the singlet phosphinidenes could be stabilized by electronic effect of the derivatives. Szieberth et al. computed the heats of formation of phosphinidenes.[7] Park and Sun[8] and Pierini and Duca[9] have studied the proton affinities, the molecular properties and the valence state of phosphinidene. Goto and Saito observed the lowest rational spectral lines of the PH radical in its ground vibronic state by submillimeter-wave spectra.[10] Examination of the lowest energy triplet and singlet electronic configuration of phosphinidene reveals their analogy with carbene. Both of them are very active and have condensation reactions with a great variety of partners.[11,12] Mathey,[13] Cowley and Barron,[14] Gonbeau and Pfister-Guillouzo,[15] and Mercier et al.[16] developed several synthetic methods for the generation and trapping of terminal phosphinidene complexes in their prolific work. They have reported the reaction mechanism of alkene addition of complex (R-P-$M(CO)_5$, R=H, ph, OCH_3, NEt_2; M=Cr, Mo, W), and found their electrophilic, carbene-like nature.

In the present work, a systematic theoretical study on the hydrogen transfer reaction of singlet thiol phosphinidene with polar molecule hydrogen fluoride is carried out in detail at the B3LYP/6-311+G (d, p) level in order to reveal the reactivity of singlet phosphinidene and the temperature effects on the reaction pathway.

COMPUTATIONAL METHODS

All DFT calculations have been carried out using the Gaussian-03 series of programs.[17] We computed the optimized geometries, total energies, and relative energies at the B3LYP/6-311+G (d,p) level. The minimum energy path (MEP) was followed in both forward direction and reverse direction using the intrinsic reaction coordination (IRC) method at the same level in order to ascertain the reaction channels better. On the other hand, by using general statistical thermodynamics and Eyring transition state theory with Wigner correction, we examined the influence of temperature on the reaction channel. All computations of the thermodynamic and kinetic parameters (ΔH°, ΔG°, ΔS°, K, k, A) were obtained in the same way as in our previous work,[18,19] and the required optimized geometries, harmonic vibration frequencies, and electronic energies are all at the B3LYP/6-311+G (d,p) level.

RESULTS AND DISCUSSION

It is well known that singlet phosphinedenes have two σ-electron pairs and one empty p-orbit in the valence shell by their electronic configurations. Then, they may be nucleophilic because of the σ-electron pairs and electrophilic because of the vacant p-orbit, and we should obtain their σ-complexes and p-complexes, respectively. These double properties can lead to reactive complexity of singlet phosphinidenes when they react with polar covalence compounds or ionic compounds. Therefore, we chose the polar molecule hydrogen fluoride forming the complex with singlet thiol phosphinidene HSP in order to examine the reactivity of the phosphinidene. The optimized structures for the initial complex reactant (**1**), the intermediate (**3**), the product (**5**), and transition states (TS**1**, **2**; TS**2**, **4**) at the B3LYP/6-311+G (d,p) level are shown in Table I. Mulliken electronic population and bond order diagram of all species are displayed in Figure 1. The calculated harmonic vibration

Table I Structure parameters of all stable species and TSs optimized at the B3LYP/6-311+G (d,p) level

Structure	Bond	Bond length (Å)	Angle	Bond angle (°)
1	F-H_a	0.9455	FH_aP	178.7
	H_a-P	2.2824	H_aPS	94.5
	P-S	2.0038	PS H_b	105.1
	S-H_b	1.3710	H_aPSH_b	180.0
2(TS**1**)	F-H_a	1.2004	PFH_a	45.6
	P-F	2.1816	SPF	101.6
	H_a-P	1.5924	PSH_b	100.1
	P-S	2.0536	H_aFPS	88.8
	S-H_b	1.3572	FPSH_b	115.2
3	F-H_a	2.2827	PFH_a	38.4
	P-F	1.6494	SPF	103.6
	H_a-P	1.4247	PSH_b	95.2
	P-S	2.1340	H_aFPS	92.5
	S-H_b	1.3494	FPSH_b	98.4
4(TS**2**)	F-H_a	2.9513	PFH_a	47.7
	P-F	1.6582	SPF	93.4
	H_a-P	2.2066	PSH_b	93.8
	P-S	2.5539	H_aFPS	−32.6
	S-H_b	1.3508	FPSH_b	192.5
5	F-P	1.6759	FPS	93.1
	S-H_a	1.3660	H_aSP	111.9
	S-H_b	1.3660	H_aSH_b	92.3
	P-S	2.2110	FPSH_a	129.0

frequencies of optimized structures are displayed in Table II. TS**1** and TS**2** each has only one imaginary frequency 1317.6i and 580.3i, respectively, which confirms the saddle point characters and corresponds to their local maximum stationary structures, i.e., TS. The others are real frequencies, suggesting their local minimum stationary structures. The total energies/the relative energies of all required species (**1**, **2**, **3**, **4**, **5**) at the B3LYP/6-311+G (d,p) level are –840.6304126 Eh/0.00 kcal/mol, –840.6060722 Eh/15.27 kcal/mol, –840.7018092 Eh/–44.80 kcal/mol, –840.5996543 Eh/19.30 kcal/mol, –840.6171956 Eh/8.29 kcal/mol, respectively. We have obtained the initial complex reactant HSPHF (**1**), and their

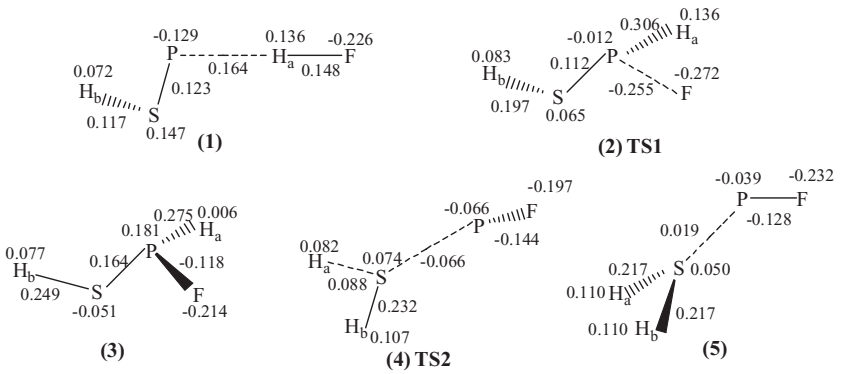

Figure 1 Mulliken electronic population and bond order diagrams of the relevant species for the hydrogen transfer reactions of singlet thiol phosphinidene complex HSP- - -HF at the B3LYP/6-311+G (d, p) level.

Table II Harmonic vibrational frequencies for all required stable species and transition states at the B3LYP/6-311+G (d, p) Level

Molecules	Frequencies (cm^{-1})
1	52.3 165.8 227.1 568.5 640.4 661.1 891.2 2459.0 3557.4
2(TS1)	1317.6i 150.5 330.1 516.4 534.4 736.5 945.0 1784.5 2592.3
3	244.2, 336.3, 474.9, 709.6, 726.1, 954.0, 986.0, 2370.3, 2667.2
4(TS2)	580.3i 101.5 153.4 267.8 528.6 733.2 1164.0 2297.9 2668.8
5	159.1 216.5 316.6 595.0 614.3 692.7 1269.3 2427.0 2495.4

complexation energies are 7.51 kcal/mol. In other phosphinidene cases such as HOP, the initial complexes is HOP—FH, which is called a p-complex and is formed by insertion of the F atom of hydrogen fluoride molecule into the P atom empty p-orbit.[18] When –SH group takes place of –OH group in singlet phosphinidene, the situation has changed. The initial complex is HSP- - -HF, and HF receives 0.090e from HSP in the initial complex reactant. Because the electronegativity of S is lower than that of O, the Mulliken electronic population of P in PSH and POH is –0.154e and –0.016e, respectively, and that of H in HF is 0.286e. So, it can be deduced that the electrostatic attraction is the main interaction form in forming the initial complex.

In the structure of TS**1**, the H_a-P/H_a-F distance and their bond orders at the B3LYP/6-311+G (d,p) level are 1.5924 Å and 0.306/1.2004 Å and –0.037, respectively, which indicates that the hydrogen atom is partially transferred from the F atom to the P atom. In the structure of TS**2**, the H_a-P/H_a-S distance and their bond orders at the same level are 2.2066 Å and 0.127/1.3845 Å and 0.088, respectively, which indicates the hydrogen atom is partially transferred from the P atom to the S atom. In order to confirm the reactants and the products connecting the obtained transition states, the IRC calculations have been undertaken at the B3LYP/6-311+G (d,p) level, the total energy and bond distance along the reaction path of step **1** and step **2** are displayed in Figures 2–5. It is obvious that the position of TS**1** is near the intermediate product region and that of TS**2** is close to the product region in Figures 2 and 3, so both of two are later barrier. The total energy of step **1** decreases very sharply after the TS**1**, while that of step 2 decreases slowly, which corresponds to what is predicted by imaginary frequencies of transition states (TS**1**: 1317i cm^{-1}; TS**2**: 580.3i cm^{-1}). From Figure 4, it is very clear that the S-H_b bond and S-P bond are almost constant along the reaction path. However, the P-F bond decreases until it reach 1.6 Å, which is just equal to the bond distance of P-F in the intermediate product **3**, the F-H_a bond distance keep constant in the reactant region, and then increase to 2.3 Å that is equal to the bond distance in **3**. From Figure 5, it can be seen that the S-H_b bond and F-P bond are almost constant along the reaction path, whereas the F-H_a bond distance increase to 3.8 Å, which means this hydrogen has been transferred. Finally, we sum up the above-mentioned analysis and find the reaction path, which is as follows:

$$\text{HSP- - -HF}(\mathbf{1}) \rightarrow \text{TS}\mathbf{1}(\mathbf{2}) \rightarrow \text{HSPH(F)}(\mathbf{3}) \rightarrow \text{TS}\mathbf{2}(\mathbf{4}) \rightarrow \text{H}_2\text{S- - -PF}(\mathbf{5}) \qquad (1)$$

Because of the different electronegativities of different substitute groups, this hydrogen transfer reaction pathway is very different from that of HOP—FH. In the case of the latter, there are two reaction paths. One is the insertion reaction [HOP—FH → three-membered ring TS →HO(H)PF], and the other is the dehydration reaction (HOP—FH →

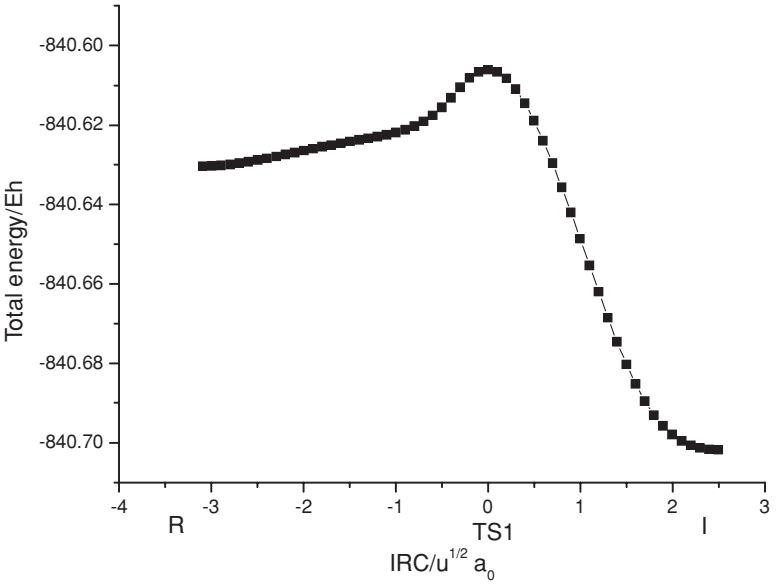

Figure 2 Total energy along the reaction path of HSP- - -HF(**1**) → TS**1** (**2,**) → HSPH(F) (**3**) (Step **1**). R, TS, and I stand for reactant region, TS region, and intermediate product region, respectively.

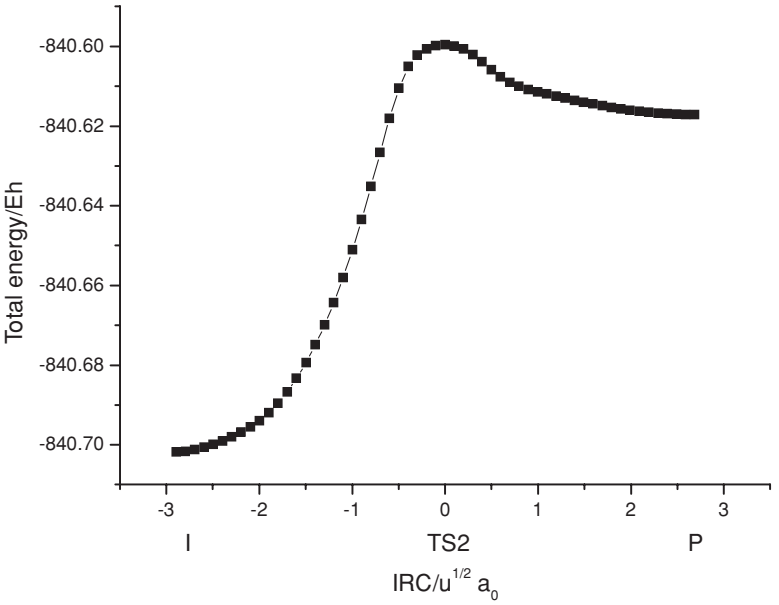

Figure 3 Total energy along the reaction path of HSPH(F) (**3**) → TS**2** (**4**) → H_2SPF (**5**) (Step **2**). I, TS and P stand for intermediate product region, TS region, and product region, respectively.

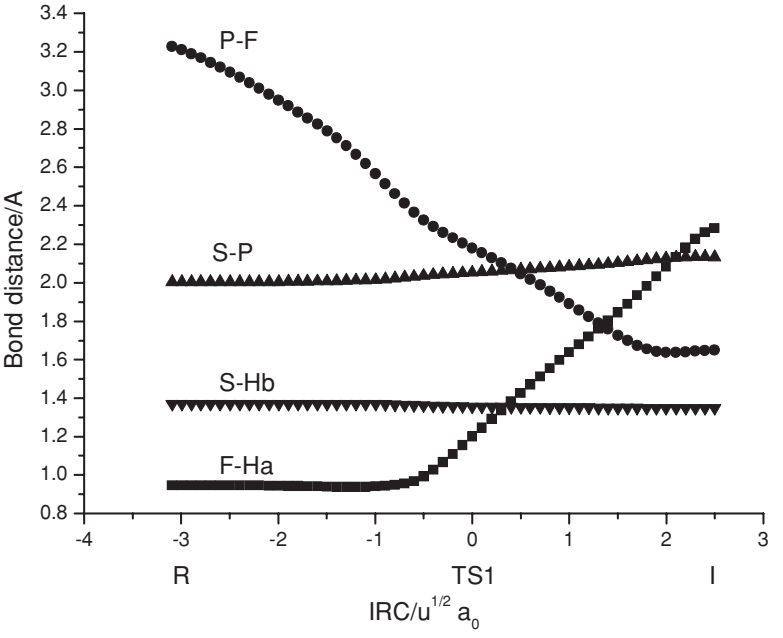

Figure 4 Bond distance along the reaction path of Step **1**. R, TS, and I stand for reactant region, TS region, and intermediate product region, respectively.

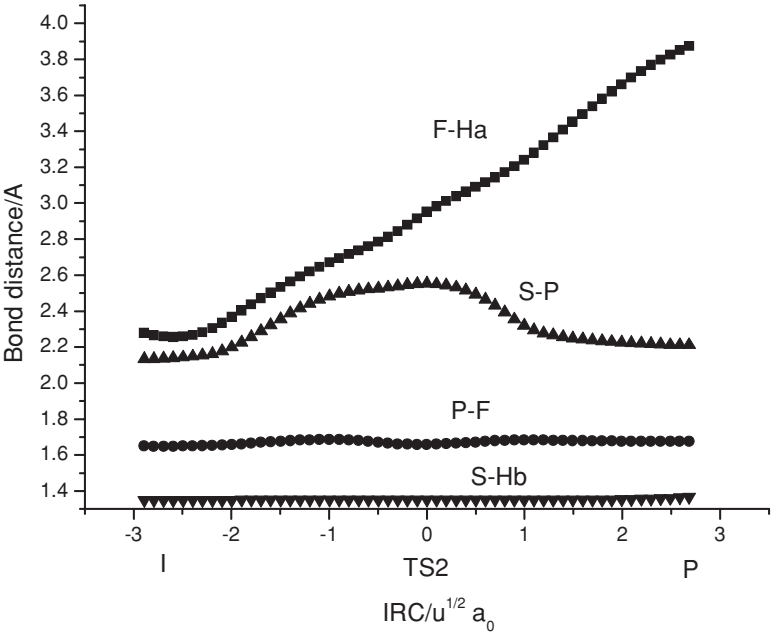

Figure 5 Bond distance along the reaction path of Step **2**. I, TS, and P stand for intermediate product region, TS region, and product region, respectively.

four-membered ring TS → H_2O + PF).[18] In this hydrogen transfer reaction pathway, the barriers of TS**1** and TS**2** are 15.27 kcal/mol and 64.10 kcal/mol, respectively. Moreover, the exoergic energies ΔE of step **1** and step **2** are correspondingly –44.80 kcal/mol and 53.09 kcal/mol. These results suggest that step **1** of the reaction [HSP- - -HF(**1**) → TS**1** (**2**) → HSPH(F) (**3**)] has both thermodynamic favor and kinetic favor, compared with step **2** [HSPH(F) (**3**) → TS**2** (**4**) → H_2SPF (**5**)].

In addition, it is known that every chemical reaction takes place at a certain temperature. In order to understand this hydrogen transfer reaction channel more deeply, we used general statistical thermodynamics and Eyring transition state theory with Wigner correction to obtain the relevant thermodynamic and kinetic data, and investigated the temperature effects. The variation of the thermodynamic and kinetic parameters with temperature is given in Table III. The enthalpy changes ΔH°, the Gibbs free energy changes ΔG°, and the entropy changes ΔS° of step **1** of the hydrogen transfer reaction are all negative in the range of 200 K–1200 K, while all relevant data of step **2** are positive. Therefore, step **1** is an exothermic and spontaneous process in which entropy decreases, while step **2** is an endothermic and non-spontaneous process in which entropy increases. In step **1**, both the enthalpy changes ΔH° and the entropy changes ΔS°decrease, but their Gibbs free energy changes ΔG° increase with the increase of temperature in the range 200 K–1200 K. On the contrary, in step **2**, both the enthalpy changes ΔH° and the entropy changes ΔS° increase, but their Gibbs free energy changes ΔG° decrease with the increase of temperature. Moreover, the equilibrium constants (K) of step **1** are very large at low temperature, but they reduce quickly with the ascend of the temperature. For example, K value is 0.389×10^{48} at 200 K and decreases to 0.246×10^{7} at 1200 K. The plot of lg$K$-1/T for step **1** and step **2** is displayed in Figure 6. From this figure, we can see that lg$K$ has a linear relationship with 1/T during the temperature, the values of step **1** decrease during the whole temperature range 200 K–1200K, while those of step **2** increase. However, the lg$K$ values of step **1** are all higher than those of step **2**. In addition, the lg$K$ differences of these reactions at low temperature are larger than those at high temperature. The order of these lg$K$ values at the every same temperature is just consistent with that of their corresponding above-mentioned exoergic energies ΔE. Therefore it is concluded that step **1** has thermodynamic favor, especially at low temperature.

In addition, we computed kinetic parameters, the A factors, and reaction rate constants. In order to reveal the probabilities of these reactions, the rate constant expression can be written as:

$$k^{TST/W} = g(k_B T/h)\exp(\Delta S_m^{/} = /R - \Delta H_m^{\#}) \tag{2}$$

$$G = 1 + 1/24/(h\nu^{\#}/k_B T)^2 \tag{3}$$

$$A = g(k_B T/h)\exp(\Delta S_m^{\#}/R) \tag{4}$$

where g is the factor corrected by Wigner; k_B and h are Bolztmann and Plank constants, respectively; R is the ideal gas constant; $\nu^{\neq}$ is the imaginary frequency of transition state; and $\Delta S_m^{\neq}$ and $\Delta H_m^{\neq}$ are standard entropy and enthalpy of activation for the system, respectively. We can find from Table III that all logA values of step **1** are nearly equal to 12 (14 for step **2**), which indicates that they all belong to the Arrhenius-type reactions. All reaction rate constants k of step **1** increase gradually during the temperature range, and those relevant values of step **2** increase sharply. For instance, it rises from 0.249×10^{-1} s^{-1} at 200 K to 0.416×10^{10} s^{-1} at 1200 K in step **1**, and it rises from 0.563×10^{-54} s^{-1} at

Table III The thermodynamic and kinetic data for Step**1** and Step**2** of the reaction during the temperature range of 200 K–1200 K

Reactions	T(K)	ΔH°	ΔG°	ΔS°	K	$k(s^{-1})$	$A(s^{-1})$
Step **1**	200	–187.84	–182.22	–28.09	0.389×10^{48}	0.249×10^{-1}	0.800×10^{12}
	400	–189.52	–175.89	–34.08	0.930×10^{23}	0.125×10^{6}	0.799×10^{12}
	600	–190.48	–168.84	–36.07	0.499×10^{15}	0.213×10^{8}	0.838×10^{12}
	800	–190.91	–161.55	–36.70	0.353×10^{11}	0.288×10^{9}	0.907×10^{12}
	1000	–191.02	–154.19	–36.83	0.113×10^{9}	0.141×10^{10}	0.985×10^{12}
	1200	–190.95	–146.83	–36.77	0.246×10^{7}	0.416×10^{10}	0.106×10^{13}
Step **2**	200	219.02	217.24	8.86	0.183×10^{-56}	0.563×10^{-54}	0.893×10^{14}
	400	220.10	215.00	12.76	0.841×10^{-28}	0.862×10^{-20}	0.237×10^{15}
	600	220.61	212.32	13.82	0.328×10^{-18}	0.265×10^{-8}	0.311×10^{15}
	800	220.88	209.51	14.22	0.209×10^{-13}	0.156×10^{-2}	0.347×10^{15}
	1000	221.07	206.64	14.42	0.161×10^{-10}	0.458×10^{1}	0.366×10^{15}
	1200	221.20	203.74	14.55	0.135×10^{-8}	0.950×10^{3}	0.377×10^{15}

ΔH°, ΔG°, and ΔS° are in units $kJ \cdot mol^{-1}$, $kJ \cdot mol^{-1}$, $J \cdot K^{-1} \cdot mol^{-1}$, respectively.

200 K to 0.950×10^3 s^{-1} at 1200 K in step **2**. The plot of lg*k*-1/T for these reaction steps is shown in Figure 6. This figure reveals that lg*k* has a linear relationship with 1/T during 200 K–1200 K, the order of these lg*k* values in agreement with that of the above-mentioned reaction barriers. All data of step **1** are larger than that of step **2**, and the lg*k* differences of these reactions at low temperature are larger than that at high temperature. Therefore, we can get a conclusion that step **1** has both thermodynamic and kinetic advantages over step **2**, and the high temperature is favorable to step **2**. In order to obtain a better understanding

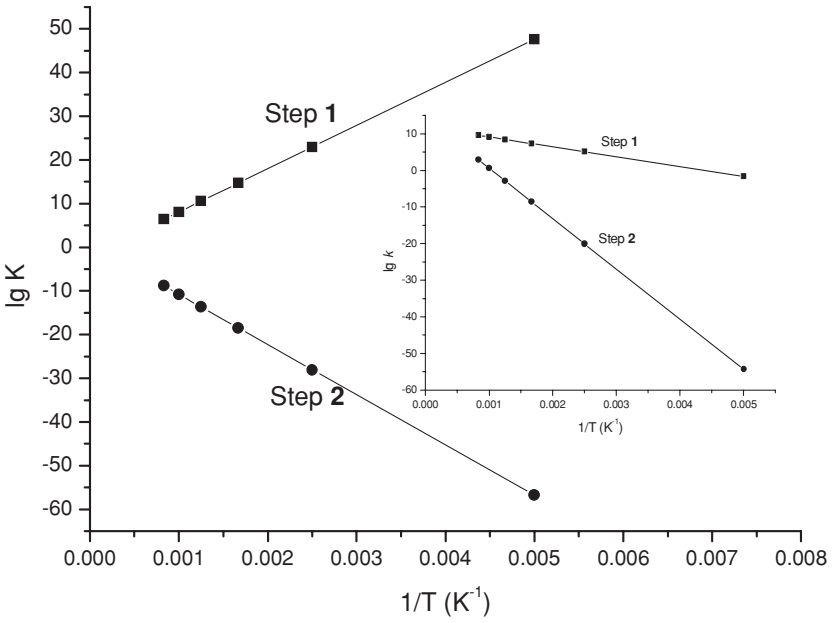

Figure 6 Plot of lg*K*- 1/T and lg*k*- 1/T (inset) for Step **1** and Step **2** of the hydrogen transfer reaction.

Table IV The thermodynamic data for the complete reaction in the temperature range 200 K–1200 K

T(K)	200	400	600	800	1000	1200
ΔH°	31.18	30.58	30.13	29.97	30.05	30.25
ΔG°	35.02	39.11	43.48	47.96	52.45	56.91
ΔS°	–19.23	–21.32	–22.25	–22.48	–22.41	–22.22

ΔH°, ΔG°, and ΔS° are in units $kJ \cdot mol^{-1}$, $kJ \cdot mol^{-1}$, $J \cdot K^{-1} \cdot mol^{-1}$, respectively.

of the whole hydrogen transfer reaction, further calculations of the thermodynamic data with different environment temperatures have been introduced in this work. As can be seen in Table IV, the entropy changes ΔS° are all negative, which means their entropy decreases over the entire temperature range. The enthalpy changes ΔH° and the Gibbs free energy change ΔG° are positive, thus, the whole hydrogen transfer reaction is endothermic and non-spontaneous. ΔG° values increase with the rise of temperature in the range 200 K–1200 K, so the reaction is favorable at low temperature.

We have investigated the reaction mechanism of the hydrogen transfer reaction of singlet thiol phosphinidene complex (HSP- - -HF) as the working reaction in order to reveal the reactivity of singlet phosphinidene and the temperature effects on the reaction pathway. Free phosphinedene has only been observed as a short-lived species in dilute gas phase or in matrices at low temperature.[5] The direct experimental measurements of the thermodynamic and kinetic parameters for the hydrogen transfer reactions of singlet thiol phosphinidene complex are especially insufficient at present. Therefore, we think that the results based on quantum calculations and thermodynamic and kinetic calculations in this work will provide useful predictions for later experimental research work.

CONCLUSIONS

From the above-mentioned detailed theoretical investigations reported in this article, we can draw the following conclusions:

1. The hydrogen transfer reaction pathway of singlet thiol phosphinidene with polar molecule hydrogen fluoride is HSP- - -HF(**1**) → TS**1** (**2**)→ HSPH(F) (**3**) → TS**2** (**4**)→ H_2S—PF (**5**), which is very different from the insertion reaction and dehydration reaction of hydroxyl phosphinidene with hydrogen fluoride.
2. Step **1** has both thermodynamic and kinetic advantages over step **2**, and the high temperature is favorable to step **2**. Moreover, the order of lg$K$ and lg$k$ for the steps is consistent with the order of their exoergic energies ΔE and barrier height of the reactions, but the differences of lg$K$ and lg$k$ for the steps decrease with the temperature increases.

The experimental information on basic spectroscopic, kinetic, and thermodynamic parameters of free phosphinidenes is very scarce for their preparative difficulty, so our research work might be useful for filling in the missing relative information.

REFERENCES

1. F. Mathey, *Multiple Bonds and Low Coordination in Phosphorus Chemistry* (Georg Thieme Verlag, New York, 1990).

2. K. B. Dillon, F. Mathey, and J. F. Nixon, *Phosphorus: The Carbon Copy* (Wiley, Chichester, UK, 1998).
3. Y. Inubushi, N. H. T. Huy, L. Richard, and F. Mathey, *J. Organomet. Chem.*, **533,** 83 (1997).
4. J. Olah, T. Veszpremi, and M. T. Nguyen, *Chem. Phys. Lett.*, **401,** 337 (2005).
5. X. Li, S. I. Weissman, T. S. Lin, P. P. Gaspar, A. H. Cowley, and A. I. Smirnov, *J. Am. Chem. Soc.*, **116,** 7899 (1994).
6. M. T. Nguyen, A. Van Keer, L. A. Eriksson, and L. G. Vanquickenborne, *Chem. Phys. Lett.*, **254,** 307 (1996).
7. D. Szieberth, T. Veszpremi, and M. T. Nguyen, *J. Mol. Struc.*, **556,** 143 (2000).
8. J. K. Park and H. Sun, *Chem. Phys. Lett.*, **195,** 469 (1992).
9. A. B. Pierini and J. S. Duca, *Int. J. Quant. Chem.*, **48,** 343 (1993).
10. M. Goto and S. Saito, *Chem. Phys. Lett.*, **211,** 443 (1993).
11. G. Frison, F. Mathey, and A. Sevin, *J. Organomet. Chem.*, **570,** 225 (1998).
12. X. Li, D. Lei, M. Y. Chiang, and P. P. Gaspar, *J. Am. Chem. Soc.*, **114,** 8526 (1992).
13. F. Mathey, *Angew. Chem. Int. Ed.*, **26,** 275 (1987).
14. A. H. Cowley and A. R. Barron, *Acc. Chem. Res.*, **21,** 81 (1988).
15. D. Gonbeau and G. Pfister-Guillouzo, *Inorg. Chem.*, **26,** 1799 (1987).
16. F. Mercier, B. Deschamps, and F. Mathey, *J. Am. Chem. Soc.*, **111,** 9098 (1989).
17. M. J. Frisch, G. W. Trucks, H. B. Schlegel, G. E. Scuseria, M. A. Robb, J. R. Cheeseman, J. A. Montgomery, Jr., T. Vreven, K. N. Kudin, J. C. Burant, J. M. Millam, S. S. Iyengar, J. Tomasi, V. Barone, B. Mennucci, M. Cossi, G. Scalmani, N. Rega, G. A. Petersson, H. Nakatsuji, M. Hada, M. Ehara, K. Toyota, R. Fukuda, J. Hasegawa, M. Ishida, T. Nakajima, Y. Honda, O. Kitao, H. Nakai, M. Klene, X. Li, J. E. Knox, H. P. Hratchian, J. B. Cross, C. Adamo, J. Jaramillo, R. Gomperts, R. E. Stratmann, O. Yazyev, A. J. Austin, R. Cammi, C. Pomelli, J. W. Ochterski, P. Y. Ayala, K. Morokuma, G. A. Voth, P. Salvador, J. J. Dannenberg, V. G. Zakrzewski, S. Dapprich, A. D. Daniels, M. C. Strain, O. Farkas, D. K. Malick, A. D. Rabuck, K. Raghavachari, J. B. Foresman, J. V. Ortiz, Q. Cui, A. G. Baboul, S. Clifford, J. Cioslowski, B. B. Stefanov, G. Liu, A. Liashenko, P. Piskorz, I. Komaromi, R. L. Martin, D. J. Fox, T. Keith, M. A. Al-Laham, C. Y. Peng, A. Nanayakkara, M. Challacombe, P. M. W. Gill, B. Johnson, W. Chen, M. W. Wong, C. Gonzalez, and J. A. Pople, *Gaussian, Inc., Pittsburgh, PA* (2003).
18. P. Yin, H. Zheng, G. Yin, J. Zhang, and S. Ye, *Mol. Phys.*, **104**(4), 599 (2006).
19. P. Yin, Y. Hu, L. Kong, P. Zhang, Q. Tang, L. Sun, and X. Xu, *Europhys. Lett.*, **77,** 23001 (2007).